# Carbon-Nanofiber-Based Nanocomposite Membrane as a Highly Stable Solid-State Junction for Reference Electrodes

Glen D. O'Neil,[†] Raluca Buiculescu,[‡] Samuel P. Kounaves,[†] and Nikos A. Chaniotakis[*,†,‡]

[†]Department of Chemistry, Tufts University, Medford, Massachusetts 02155, United States

[‡]Laboratory of Analytical Chemistry, Department of Chemistry, University of Crete, 71 003 Iraklion, Crete, Greece

ABSTRACT: There is currently a need for a reliable solid-state reference electrode, especially in applications such as autonomous sensing or long-term environmental monitoring. We present here for the first time a novel solid-state nanofiber junction reference electrode (NFJRE) incorporating a junction consisting of poly(methyl methacrylate) and carbon graphene stacked nanofibers. The NFJRE operates by using the membrane polymer junction, which has a very high glass transition temperature (T_g) and small diffusion coefficient, to control the diffusion of ions, and the carbon nanofibers lower the junction resistance and act as ion-to-electron transducers. The fabrication of the NFJRE is detailed, and its behavior is characterized in terms of its impedance, stability, and behavior in comparison with traditional reference electrodes. The NFJRE showed a response of $<5-13$ mV toward a variety of electrolyte solutions from 10^{-5} to 10^{-2} M, <10 mV over a pH range of $2-12$, and excellent behavior when used with voltammetric methods.
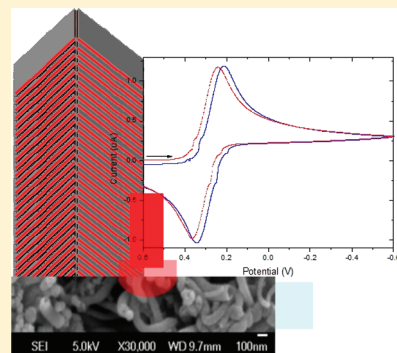
A reference half-cell, or electrode, serves two main functions in an electrochemical cell: it establishes a stable half-cell potential that is independent of sample solution, and together with the working and counter electrodes, it completes the electrochemical cell.[1,2] Common reference electrodes based on Ag/AgCl or Hg/Hg$_2$Cl$_2$ require an aqueous electrolyte junction to be in contact with the sample. Unfortunately, these electrodes have several drawbacks, making their application cumbersome for long-term or remote autonomous sensing applications. They are difficult to miniaturize, can contaminate the sample as the internal electrolyte diffuses into the test solution, have restrictions regarding their geometry and position during measurement, and require frequent replenishment of the inner-filling solution as well as unclogging of the reference junction.[3,4]

There have been many advances in the field of chemical sensor technology, including miniaturization and improvements in the detection limit and selectivity. In particular, solid-state ion-selective electrode (SS-ISE) technology has eliminated the need for a liquid inner-filling solution by replacing it with new electro-active materials, such as conductive polymers or polymeric hydrogels.[5-7] Such solid-contact ISEs are ideal for autonomous and remote sensing applications, as recently shown by their use as the wet chemistry laboratory (WCL) on board NASA's 2007 Phoenix Mars Lander.[8,9] However, the lack of a suitable reference electrode in this case required the WCL sensors to be referenced to a lithium ISE half-cell with addition of 0.001 M LiNO$_3$ as a stable background electrolyte.[9] Two problems arose from this choice: the first was the assumption that there was no soluble lithium in the Martian soil, and second, the use of the LiNO$_3$ precluded the detection of NO$_3^-$ below 0.001 M.

Analogous to the recent advances seen in SS-ISE research, there have also been advances in the design and implementation of solid-state reference electrodes, particularly the elimination of

an inner filling solution and, thus, a liquid junction.[1,3,10-18] In general, all of the currently available solid-state-based electrodes (sensors and references) have an inner solid, conductive, redox-active support as a common design element that is coupled with either an outer reversible redox buffering system or a nonselective polymeric membrane.[10] Several groups have reported solid-state junction designs for reference electrodes using polymers doped with lipophilic additives[11,12] or ionic species[1,3,8] as well as using conductive polymers[14,15] and ionic liquids[16,17] immobilized on solid supports. Kwon et al. implemented a layer-by-layer polymer approach to obtain a reference electrode for blood gas analysis.[1] In that work, silicone rubber was impregnated with KCl and covered with a Nafion cation exchange resin to prevent leaching of chloride anions. This reference half-cell showed minimal response toward a variety of charged electrolytes and pH. However, a layer-by-layer approach is known to produce sensors with very high resistance, and the KCl is expected to partition into the test solution.

Mattinen et al. fabricated a reference electrode, based on polyvinylchloride (PVC) membranes doped with combinations of lipophilic salts, that showed high potential stability but very slow response time.[18] This sensor was tested only against chloride, which is unusual, given the large amount of lipophilic additives in the membrane. Kisiel et al. have shown that doping the polymer poly(n-butyl acrylate) with the lipophilic salt ETH 500 yields an electrode that is relatively nonresponsive to KCl, NaCl, and NaNO$_3$.[12] Recently, this membrane was prepared as part of an electrode that used carbon nanotubes as the ion-to-electron transducer.[19] However, there are three assumptions that

must be true for the lipophilic salt-based reference half cells to maintain a stable reference potential in different test solutions and over time: (1) The lipophilicity of both the anion and the cation of the salt employed (such as ETH 500) must be the same; (2) the chemical stability and the diffusion coefficients of the anion and cation of the lipophilic salt must be identical within the sensing membrane; and (3) the lipophilicity of the analyte ion pairs in the test solution must be balanced, since any changes in the lipophilicity of the analyte ions will be measured as a response of the reference half cell.[20] These assumptions are so far-reaching that they are almost impossible to realize in a real life analytical system and during the duration of a measurement with fluctuating activities. Thus, such reference half cells cannot perform at levels that will allow their widespread application in autonomous sensing systems.

Recent studies highlighting the advantages of carbon nanomaterials, such as nanotubes, fullerenes, and nanofibers, as efficient ion-to-electron transducers in biosensors have shown that these materials have stable, reproducible potentials due to the large double-layer capacitance arising at the interface of the transducer and membrane.[21−27] Nanofibers differ from nanotubes or fullerenes in that their structure is that of stacked graphene layers. They possess mechanical and electrical properties similar to carbon nanotubes[28] and, in addition, have a very large number of active sites, which originate from the exposed graphene edges found throughout the surface of the nanofibers. The degree of functionalization on the surface of the nanofibers can be easily controlled, leading to predictable behavior in the sensing element.[21,29]

Here, we describe the immobilization of nanofibers in a nonplasticized polymer with a high glass transition temperature (T_g) to limit the mobility of ions in the membrane. The polymer of choice is poly(methyl methacralate) (PMMA) with T_g = 90−110 °C and very low water absorption (∼27 $\mu g/mm^3$).[30] This polymer also has a very small diffusion coefficient compared with water, eliminating the possibility for generating a potential due to ion diffusion.[30] The required stable redox current is maintained by limiting the amount of ionic flow through the membrane, while the ion-to-electron transduction and completion of the electrochemical circuit is achieved by the carbon nanofibers. The amount of nanofibers incorporated will determine the resistance of the reference half cell, and, thus, can be adjusted to a level suitable for typical measurement systems. In addition, the resistance of the membrane allows for improvements in reference electrode miniaturization. In this paper, we use these unique materials to fabricate and demonstrate their use in a solid-state, nanofiber junction reference electrode (NFJRE).

■ MATERIALS AND METHODS

Reagents. Poly(methyl methacralate), *m*-xylene, potassium chloride, sodium chloride, ammonium chloride, calcium chloride, potassium nitrate, potassium perchlorate, potassium iodide, and magnesium perchlorate were purchased from Sigma. Carbon nanofibers (CNFs) were purchased from Electrovac AG (Austria). All solutions were prepared using 18.2 MΩ-cm^{-1} water (Barnstead Nanopure, Massachusetts).

SEM. Scanning electron microscopy images of samples were obtained using a JEOL 7000 scanning microscope in SE mode. Previous to scanning electron microscopy (SEM) imaging, a 10 nm Au layer was deposited on the samples through spin-coating.
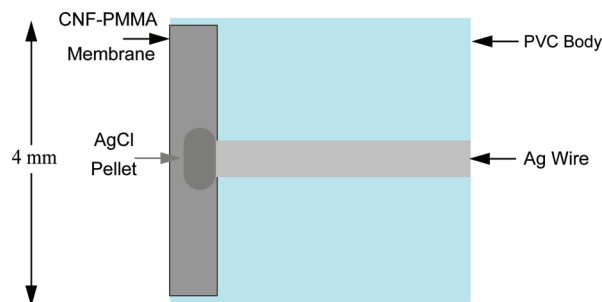
Figure 1. Diagram showing the construction of the nanofiber junction reference electrode (NFJRE).

Electrochemical Measurements. Potentiometric measurements were conducted using an Orion model 555A with measured input impedance of 5×10^{12} Ω in conjunction with an Orion model 607 switchbox (Orion, Bedford, MA). Concentrations were adjusted using a standard addition from 10^{-5} M solutions. Measurements were made in a 5 min cycle in unstirred solutions: the potential difference was allowed to stabilize for 3 min before data was recorded every 15 s during the final 2 min. Commercial potassium and nitrate ion-selective electrodes were obtained from Electrochemical Analytical Systems (Iraklion, Crete, Greece). A single-junction reference electrode (model RE-5B) from BASi (West Lafayette, IN, USA) and an Orion sure-flow, double-junction reference electrode (model 900200) from Thermo Scientific (Bedford, MA, USA) were used in comparative studies.

The impedance spectra were generated using a three-electrode system with a Ag/AgCl (3 M KCl) half cell as reference, platinum disk counter electrode, and an Autolab PGSTAT 30 potentiostat/galvanostat equipped with a frequency response analyzer module (Eco Chemie, Netherlands). Resistance was measured by scanning current between ±1 pA and recording the resulting potential using a Keithley model 6430 electrometer with the NFJRE as a working electrode and a platinum wire as the reference/counter.

Electrode Construction. A schematic of a NFJRE is shown in Figure 1. Electrode bodies were assembled by heating a 1-mm-diameter Ag wire (AlphaAesar, 99.999% purity) to approximately 900 °C and dipping into molten AgCl for several seconds until a 2 mm pellet formed at the tip of the wire to act as the internal reference element. This Ag/AgCl pellet was then epoxied into an in-house fabricated PVC electrode body. The nanocomposite membrane was prepared by dissolving 9 parts PMMA and 1 part CNF in *m*-xylene. The mixture was sonicated for 10 min before applying to the electrode body in 30 μL aliquots.

■ RESULTS AND DISCUSSION

Nanofibers play a dual role in the operation of the reference junction by providing ion-to-electron redox transduction and lowering membrane resistance. The redox chemistry is provided by the nanofibers' numerous surface functionalities, such as ketones, carboxylic acids, and ethers. The nanofibers' high conductivity reduces the membrane resistance to values compatible with typically available potentiometric measurement systems (R < 10 MΩ). The polymer interface with the Ag|AgCl redox couple provides a stable contact between the junction and the electronics.
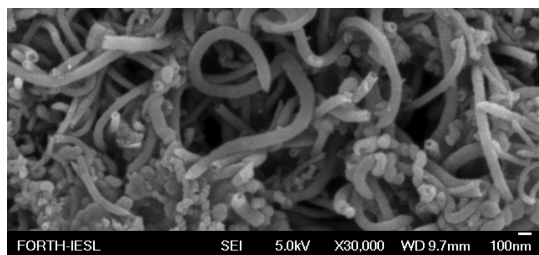
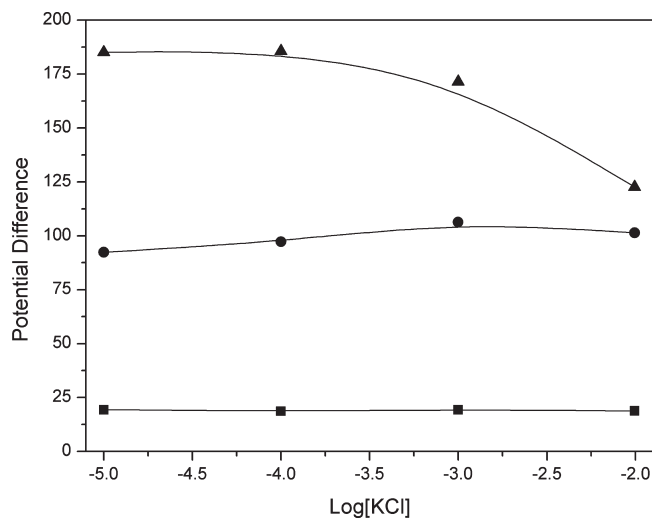**Figure 2.** Scanning electron microscopy image of a CNF/PMMA membrane.
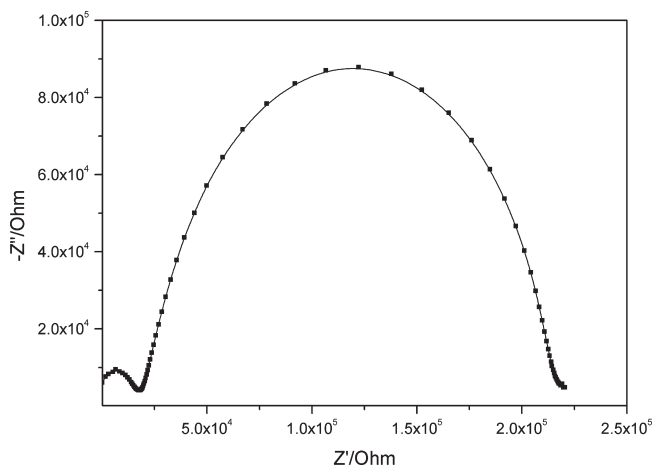
Figure 3. An impedance plot of the NFJRE in 0.1 M KCl. Frequency range $0.01-10^6$ Hz; amplitude, 50 mV; reference electrode, Ag|AgCl half cell; counter electrode, Pt disk.


Figure 4. Response of sensors with different nanocomposite membranes to potassium chloride: (▲) LHT, (●) GFE/LHT, and (■) HTE nanocomposite membranes. Potential difference (mV) vs an Orion sure-flow, double-junction reference electrode.

For all studies, 10 wt % of nanofibers was used for the construction of the reference junctions. This ensures that the solution was saturated with CNFs and, as shown in the SEM image of the membrane in Figure 2, that the required contact between individual fibers was present.

The impedance of the reference junction was quantitatively determined using electrochemical impedance spectroscopy and dc scanning current resistance measurements (Figure 3). The spectrum shows two distinct impedance regions: one at the junction/solution interface (low frequency) and the other at the Ag|AgCl redox couple (high frequency). The absence of a Warburg diffusion region is very evident. As suspected, this clearly shows that there is no electrolyte diffusion within the membrane, due to the absence of both a plasticizer and lipophilic additive.

There are three different grades of nanofibers that can be used for fabricating the solid-state junction, designated as HTE, LHT, and GFE.[21] The major differences among these fibers are due to the different physical and chemical postsynthesis treatments and have been previously described.[21] The three grades employed here differ in the number of active sites and, in particular, the acidic and basic groups. The number of acidic and basic functionalities is especially important in understanding the surface chemistry of carbon materials.[31] It has been reported that functional groups such as carboxyls, lactones, and phenols contribute to the acidic character, whereas pyrones, ethers, chromenes, and carbonyls contribute to the basic character.[21,31]

Three electrodes were constructed using each type of nanofiber, and their performance was evaluated by measuring their potential (vs a commercial double-junction reference) using increasing concentrations of KCl as a model system. As shown in Figure 4, the type of nanofiber drastically influences both the starting potential and the overall response. The starting potential and response toward KCl increases in the order of HTE < GFE < LHT. This trend is related to the acidity/basicity of the nanofibers. It has been shown that LHT fibers contain the largest number of acidic groups and are responsible for negative response from increasing chloride ion concentration. In contrast, the GFE fibers have a high concentration of basic groups and are responsible for the positive response from the potassium ions. We believe that a balance of acidic and basic constituents on the surfaces of the HTE nanofibers is responsible for the absence of any response.

The most important characteristic of a reference cell is the absence of any response toward electrolytes and pH. Figure 5 shows the electrode response toward various electrolyte solutions over the concentration range from 10^{-5} to 10^{-2} M. A very small response (typically at $>10^{-4}$ M) of 5–6 mV was observed for most electrolytes, with the exception of $CaCl_2$, which showed a response of 13 mV. This response, though greater than that for the other ions, is still relatively small, considering the wide range of concentrations tested.

The response of these electrodes was also compared with that of two commercial reference electrodes. In this experiment, the potentials of K$^+$ and NO$_3^-$ ISEs, BASi single-junction reference, and the NFJRE were measured against an Orion sure-flow double-junction reference electrode. The potentials of the reference electrodes were then subtracted from the signal of the ISE, and a constant was added to each so that the starting potentials were identical: $E = (E_{DJ} - E_m) + C$, where E is the reported potential, E_{DJ} is the potential of the ISE measured against a double-junction reference, E_m is the potential of the ISE measured against another reference, and C is a constant. Data presented in this manner facilitates comparison of the potentials of the reference electrodes on the measured potential from the
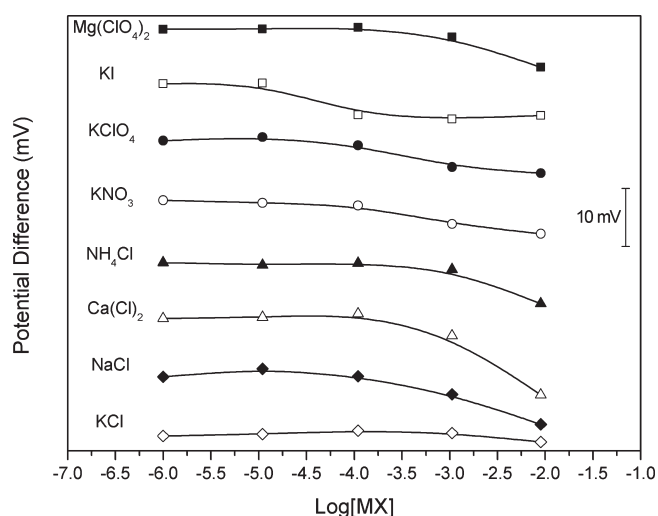
Figure 5. Electrode response to salt solutions in the range from 10^{-5} M to 10^{-2} M. All potentials were referenced to an Orion model 900200 double-junction reference electrode.

Table 1. Comparison of Recovery of K^+ and NO_3^- Obtained Using an Orion Sure-Flow, Double-Junction (DJ), a NFJRE, and a BASi Ag|AgCl Single-Junction, As References for the K^+ and NO_3^- ISEs

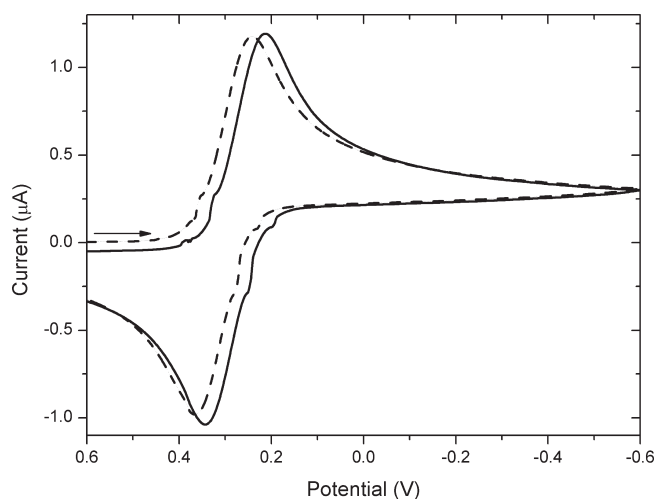|		[K^+]		[NO_3^-]	
	[KNO_3] added (M)	measured (M)	recovery (%)	measured (M)	recovery (%)
vs Orion DJ	1.09×10^{-3}	1.06×10^{-3}	97.2	1.07×10^{-3}	97.8
vs NFJRE		1.08×10^{-3}	98.6	1.0×10^{-3}	96.2
vs BASi		1.06×10^{-3}	97.2	1.06×10^{-3}	97.2

ISE. The results show that the NFJRE behaves similarly to the commercial reference cells. Calibration curves for K^+ and NO_3^- obtained using the NFJRE are almost identical to those obtained using the two commercial reference electrodes. The largest difference in potential occurs at 10^{-1} M KNO_3^-, which is 3 mV for K^+ and 4 mV for NO_3^-. These responses induce an error in the measured concentration of <3%. The recovery of potassium and nitrate using the various electrodes and the two ISEs is shown in Table 1.

A major concern when using carbon nanomaterials as a junction is their sensitivity to pH due to the many oxygen-containing functional groups on their surfaces.[21,22,31] The pH sensitivity of the NFJRE was evaluated in aqueous solutions with a pH range between 2 and 12, adjusted by adding KOH to a 0.01 M HCl solution. As can be seen in Figure 6, the HTE-based NFJRE shows a response of <10 mV over the entire pH range tested (10 orders of magnitude). The results show very little influence on the measured potential of the solid-state reference when compared with commercial references.

The use of the NFJRE for dynamic potential scanning techniques was verified using cyclic voltammetry (CV) of the $K_3[Fe(CN)_6]/K_2[Fe(CN)_6]$ redox couple and compared with a CV obtained using a commercial double-junction reference electrode. As shown in Figure 7, the two CV peaks are offset by 26 mV, corresponding to the potential difference between the
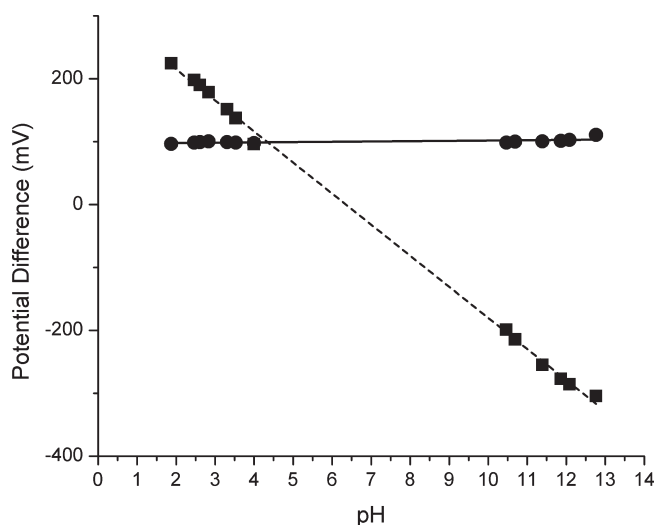
Figure 6. Electrode response to pH. The response of the NFJRE is displayed with a solid line between pH 2 and ~13. The response of a pH electrode versus an Orion sure-flow, double-junction reference electrode is plotted over the same range (dotted line). Data points are averages of three measurements. The error bars in each measurement are less than 1.5 mV and, thus, do not appear on the plot.


Figure 7. Cyclic voltammogram of 1 mM $K_3[Fe(CN)_6]/K_4[Fe(CN)_6]$ in 1.0 M KNO_3. The scan start and direction is indicated by the arrow. Reference electrode, commercial double-junction (solid line) and NFJRE (dotted line); working electrode, 3 mm glassy carbon ($A = 0.07$ cm^2); counter electrode, Pt wire.

two reference electrodes. The reduction and oxidation peaks are separated by approximately the same potential difference for both electrodes. The potential of the solid-state junction remained stable and had very little influence on the measured current, indicating that this electrode can also be successfully used for voltammetric/amperometric measurements.

The medium-term stability of the NFJRE was evaluated by monitoring the potential in 0.1 M KCl over a four-day period of continuous operation (Figure 8). The NFJRE showed a 5 mV drift during this measurement window, although there were small fluctuations in the short term potential of 1−2 mV, which is within experimental error margins. The reproducibility was evaluated by measuring six identical electrodes in 0.1 KCl and
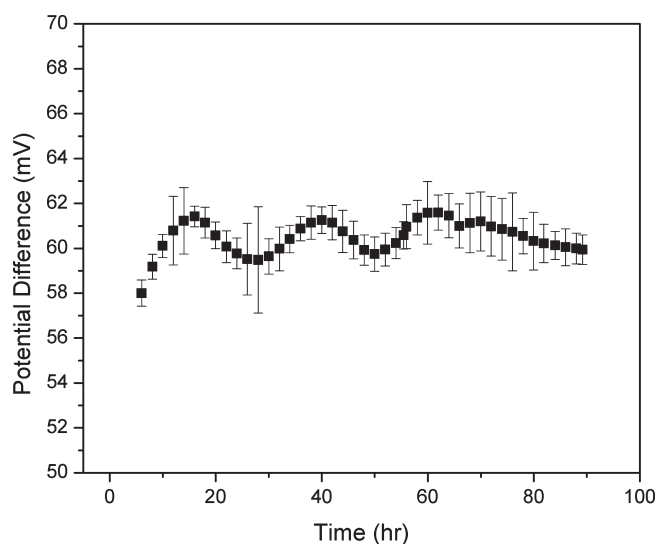
Figure 8. Potential measurement of a NFJRE versus a double-junction reference in 0.1 M KCl over 90 h of continuous operation. Each point represents the average potential measured over 1 h with error bars corresponding to the maximum and minimum potentials measured during the time window.

comparing their starting potentials. The average of these measurements was 75.6 ± 3.9 mV ($n = 6$). The response time of the electrodes was very fast; the potential of the cell stabilized within a few seconds.

■ CONCLUSIONS

In this work, we have presented for the first time the use of a polymer−carbon nanofiber nanocomposite as a junction for solid-state reference electrodes. A highly stable and reproducible potential is obtained by employing a polymer with a high T_g and small diffusion coefficient, and the graphene layered carbon nanofibers decrease the membrane resistance and provide the required ion to electron transfer mechanism. The potential of this electrode is not influenced by any common electrolytes or pH, making it an ideal solid state reference electrode that can be used in conjunction with a variety of chemical and biochemical sensors and electrochemical techniques, such as potentiometry and voltammetry.

■ AUTHOR INFORMATION

Corresponding Author
*E-mail: nikolaos.chaniotakis@tufts.edu.

■ ACKNOWLEDGMENT

■ REFERENCES

(1) Kwon, H. -K.; Lee, K. S.; Won, M. S.; Shim, Y. B. *Analyst* **2007**, *132*, 906–912.

(2) Bard, A. J.; Faulkner, L. R. *Electrochemical Methods*, 2nd ed.; Wiley: New York, 2001.

(3) Nolan, M. A.; Tan, S. H.; Kounaves, S. P. *Anal. Chem.* **1997**, *69*, 1244–1247.

(4) Guth, U.; Ferlach, F.; Decker, M.; Oelssner, W.; Vonau, W. *J. Solid State Electrochem.* **2009**, *13*, 27–39.

(5) Bobacka, J.; Ivaska, A.; Lewenstam, A. *Electroanalysis* **2003**, *15*, 366–374.

(6) Bobacka, J.; Ivaska, A.; Lewenstam, A. *Chem. Rev.* **2008**, *108*, 329–351.

(7) Lukow, S. R.; Kounaves, S. P. *Electroanalysis* **2005**, *17*, 1441–1449.

(8) Kounaves, S. P.; Hecht, M. H.; West, S. J.; Morookian, J.; Young, S. M. M.; Quinn, R.; Grunthaner, P.; Wen, X.; Weilert, M.; Cable, C. A.; Fisher, A.; Gospodinova, K.; Kapit, J; Stroble, S.; Hsu, P.; Clark, B. C.; Ming, D. W.; Smith, P. H. *J. Geophys. Res.* **2009**, *114*, E00A19, doi:10.1029/2008JE003084.

(9) Hecht, M. H.; Kounaves, S. P.; Quinn, R. C.; West, S. J.; Young, S. M. M.; Ming, D. W.; Catling, D. C.; Clark, B. C.; Boynton, W. V.; Hoffman, J.; DeFlores, L. P.; Gospodinova, K.; Kapit, J.; Smith, P. H. *Science* **2009**, *325*, 64–67.

(10) Kisiel, A.; Marcisz, H.; Michalski, A.; Maksymiuk, K. *Analyst* **2005**, *130*, 1655–1662.

(11) Anastasova-Ivanova, S.; Mattinen, U.; Radu, A.; Bobacka, J.; Lewenstam, A.; Migdalski, J.; Danielewski, M.; Diamond, D. *Sens. Actuators, B* **2010**, *146*, 199–205.

(12) Kisiel, A.; Michalska, A.; Maksymiuk, K.; Hall, E. A. H. *Electroanalysis* **2008**, *20*, 318–323.

(13) Desmond, D; Lane, B.; Alderman, J.; Glennon, J. D.; Diamond, D.; Arrigan, D. W. M. *Sens. Actuators, B* **1997**, *44*, 389–396.

(14) Chen, C. C.; Chou, J. C. *Jpn. J. App. Phys.* **2009**, *48* (111501), 1–6.

(15) Mangold, K. M.; Schäfer, S.; Jüttner, K. *Fresnius' J. Anal. Chem.* **2000**, *367*, 340–342.

(16) Mamińska, R.; Dybko, A.; Wróblewski, W. *Sens. Actuators, B* **2006**, *115*, 552–557.

(17) Kakiuchi, T.; Yoshimtsu, T.; Nishi, N. *Anal. Chem.* **2007**, *79*, 7187–7191.

(18) Mattinen, U.; Bobacka, J.; Lewenstam, A. *Electroanalysis* **2009**, *21*, 1955–1960.

(19) Rius-Ruiz, F. X.; Kisiel, A.; Michalska, A.; Maksymiuk, K.; Riu, J.; Rius, X. F. *Anal. Bioanal. Chem.* **2011**, *399*, 3616–3622.

(20) Dinten, O.; Spichiger, U. E.; Chaniotakis, N.; Gehrig, P.; Rusterholz, B.; Morf, W. E.; Simon, W. *Anal. Chem.* **1991**, *63*, 596–603.

(21) Vamvakaki, V.; Tsagaraki, K.; Chaniotakis, N. *Anal. Chem.* **2006**, *78*, 5538–5542.

(22) Stavyiannoudaki, V.; Vamvakaki, V.; Chaniotakis, N. *Anal. Bioanal. Chem.* **2009**, *395*, 429–435.

(23) Vamvakaki, V.; Chaniotakis, N. *Sens. Actuators, B* **2007**, *126*, 193–197.

(24) Parra, E. J.; Crespo, G. A.; Riu, J.; Ruiz, A.; Rius, F. X. *Analyst* **2009**, *134*, 1905–1910.

(25) Zelada-Guillén, G. A.; Bhosale, S. V.; Riu, J.; Rius., X. F. *Anal. Chem.* **2010**, *82*, 9254–9260.

(26) Lai, C.-Z.; Joyer, M.; Fierke, M.; Petkovich, N.; Stein, A.; Bühlmann, P. *J. Solid State Electrochem.* **2009**, *13*, 123–128.

(27) Collins, P. G.; Arnold, M. S.; Avouris, P. *Science* **2001**, *292*, 706–709.

(28) Endo, M.; Kim, Y. A.; Hayashi, T.; Fukai, Y.; Oshida, K.; Terrones, M.; Yanagisawa, T.; Higaki, S.; Dresselhaus, M. S. *Appl. Phys. Lett.* **2002**, *80*, 1267–1269.

(29) Merkulov, V. I.; Hensley, D. H.; Guillorn, M. A.; Lowndes, D. H.; Simpson, M. L. *J. Phys. Chem. B* **2002**, *106*, 10570–10577.

(30) Unemori, M.; Matsuya, Y.; Matsuya, S.; Akashi, A.; Akamine, A. *Biomaterials* **2003**, *24*, 1381–1387.

(31) Lopez-Ramon, M. V.; Stoeckli, F.; Moreno-Castilla, C.; Carrasco-Marin, F. *Carbon* **1999**, *37*, 1215–1221.

5753

dx.doi.org/10.1021/ac201072u |*Anal. Chem.* 2011, 83, 5749–5753